CR-152403

(K Aoyagi)

4

(NASA-CR-152403) STATIC TESTS OF THE J97 POWERED, EXTERNAL AUGMENTER V/STOL WIND TUNNEL MODEL (De Havilland Aircraft Co. of Canada Ltd.) 44 p HC A03/MF A01 CSCL 01A

N81-21010

Unclas

G3/02 16385

DH

CANADA

THE DE HAVILLAND AIRCRAFT OF CANADA LIMITED

NASA CR 152403

DHC-DND 77-4

STATIC TESTS OF THE J97 POWERED, EXTERNAL AUGMENTOR V/STOL WIND TUNNEL MODEL AT DHC

FEBRUARY, 1978

THE DE HAVILLAND AIRCRAFT OF CANADA LIMITED

DHC-DND 77-4

STATIC TESTS OF THE J97 POWERED, EXTERNAL AUGMENTOR V/STOL WIND TUNNEL MODEL

NASA Contract No: NASW 2797
DSS Contract Serial No: 2SR5 - 0012

Prepared by. D. B. Garland ....
D. B. Garland

Approved by. D. C. Whittley ....
D. C. Whittley

1. SUMMARY

The J97-powered, external-augmentor, large-scale, V/STOL model was successfully tested in the static mode (zero forward speed) at DHC in November/December 1977.

With a ground clearance of 7.5 feet, believed to have put the model essentially out of ground effect, a gross thrust augmentation ratio of 1.60 at NPR = 3.0 was measured for the fuselage augmentor. A similar figure was apparent for the wing augmentor.

An overall ratio of model thrust to bare engine thrust of 1.52 was determined at NPR = 3.0.

The structural integrity of the model was well demonstrated and duct pressure losses were small.

Wind tunnel tests are scheduled for February/March 1978 in the 40 x 80 ft. wind tunnel at the Ames Research Center, NASA.

2. CONTENTS

3. INTRODUCTION

The external-augmentor concept for V/STOL aircraft has been the subject of research at DHC on a modest level of effort for more than ten years. A description of the concept, early research and possible applications was given in Reference 1.

The present program includes the design, manufacture and test of a large-scale model powered by a G. E. J97 jet engine. This report covers static tests of the model at DHC prior to shipment to NASA, Ames for tests in the 40 x 80 foot wind tunnel.

Funding restraints and the need to minimize the number of hours put on the J97 have resulted in a rather limited, first, static test program. More extensive static tests are planned for the period after the first wind tunnel tests when modifications and configurations actually tested at forward speed can be tested statically. Nevertheless, some very encouraging results were obtained from the first tests and have provided the necessary confidence that both mechanical and aerodynamic performance are sufficient to embark upon the wind tunnel tests.

4. DESCRIPTION OF MODEL

4.1 General Arrangement

A G.A. drawing of the model is shown in Figure 1. It is a "conceptual model" with the main feature being that vertical jet lift is provided by two fore and aft ejectors located on either side of the fuselage. The need to achieve approximate coincidence of jet lift, aerodynamic centre and c.g. leads to the choice of a double delta type planform as described in Reference 1. Approximately twenty percent of the thrust is used to power a trailing edge augmentor flap which is deflected to 90^{o} for hover and which provides thrust vectoring for transition.

A review was made of the engines available for the model and a single GE J97 was chosen primarily because it operates with a high jet pipe (or nozzle) pressure ratio (PR = 3). The choice of a single engine for the model suggested that it could be considered more representative of fighter type aircraft (rather than a multi-engine transport as shown in Reference 1) and therefore some care was taken to maintain a low frontal area and a reasonable thrust loading (based on the planform area of the wing).

The model will be fitted with a conventional empennage with high tail for the wind tunnel tests although it is recognized that a canard (or foreplane) may eventually become a more appropriate choice (depending upon the longitudinal trim results to be obtained from the wind tunnel). *Figure 2 is a photograph of the model on its test rig.

In the concept the augmentor shrouds (or doors) are intended to retract as shown in Figure 3 and furthermore, closing these doors would take place progressively during transition from hover to forward flight - the purpose being to reduce secondary flow and momentum drag. In the model, this feature has been accommodated to a very limited extent such that only one partially closed configuration is possible - modifications to the model would permit a much wider range of positions for the future.

For the present, only minimal provisions have been incorporated in the model to represent reaction controls for use in hover and transition. Again, this could become an important aspect of a future test program. Nevertheless, some provisions have been made to achieve longitudinal trim and a positive thrust/drag margin throughout transition - this is achieved by blanking off flow to some of the fuselage augmentor nozzles and increasing the propulsion nozzle accordingly.

Table I lists the major geometric parameters of the airframe.

4.2 J97 Performance

The original performance information on the J97 (from NASA, Ames in January 1974) indicated a static thrust of about 5500 lb. at an exhaust gas pressure ratio of 3.5. The particular engine made available for the present tests appears to have a higher EGT than expected so that even with an enlarged effective nozzle area it produces only about 4900 lb. of thrust at $N/\sqrt{\theta} = 100\%$.

4.3 Fuselage Augmentor

The design of the fuselage augmentor is based on laboratory development of high aspect ratio, segmented nozzle augmentors, a process which culminated in full-scale but cold flow tests of a section of the VTOL model augmentor.

A section through the augmentor is shown in Figure 3. Its geometry is defined in Table 2. The duct which supplies exhaust gas to the fuselage augmentor nozzles is shown in Figure 4.

The nozzles for the fuselage augmentor have been designed to give an essentially vertical jet efflux. The spanwise momentum of the flow in the nozzle is counteracted by the sweep angle of the nozzle exit plane, which varies from 17^o at the inboard end to 0^o at the outboard end. Figure 5 shows the nozzle.

The location of the nozzles in the augmentor is arranged to give some BLC effect on the diffuser walls and on the augmentor end walls.

4.4 Wing Augmentor

The wing augmentor is designed around a nozzle array with AR = 40 nozzles, a pitch spacing ratio $p/t = 8$ and a total nozzle exit area of 11.5 in^2 per wing. The supply duct has been made as large as possible, within the wing profile, in order to simplify the nozzle/duct junction, i.e., a low duct Mach number, less than 0.18, allows the use of a sharp-edged junction without excessive pressure losses. Figure 6 shows a typical section through the wing augmentor. It is made in three bays, as indicated in Figure 1, with constant geometry nozzles in each bay. Optimum augmentor throat size occurs, therefore, at only one spanwise station in each bay (since the shrouds are linearly tapered across the whole span). The augmentor length ratio $L/\bar{t}$ averages 90 across the span.

4.5 Rear Fuselage Nozzle

A small trimming nozzle is used to obtain the optimum J97 effective nozzle area. A simple sharp-edged orifice is used whose discharge coefficient and thrust efficiency characteristics were determined from cold flow laboratory tests.

This nozzle can be increased in size when the wing augmentor is not used or to other sizes for cases when only the wing augmentor is used or when neither augmentor is used, i.e., the simple, straight-through case, although, the latter is not planned for the present test series.

4.6 Wing

A six percent thick, double-delta wing was chosen to provide sufficient volume for the augmentor nozzles and to give an aerodynamic centre somewhere aft of the static centre of lift.

Typical engine inlet locations adjacent to the fuselage at the leading edge of the wing have been replaced by simple fairings.

The wing augmentor-flap can be rotated through 0^{o} to 90^{o} deflection angle.

4.7 Empennage

A typical fin and tailplane have been built for the wind tunnel tests to provide some measure of directional and longitudinal stability but they were not installed for the static tests. The G.A. of Figure 1 shows the empennage and Table 1 gives further details.

5. DESCRIPTION OF TESTS

5.1 Test Rig

A simple test rig, which doubled as an assembly stand and a transport trolley, was built to suit the model. The three support strut locations were the same as those to be used in the wind tunnel. The support strut lengths were such as to give a ground clearance of 7.5 feet under the fuselage augmentor, a dimension derived from previous tests of a similar configuration model to put the present model out of ground effect. The rear struts (see Figure 7) were wire braced back to ground and the front strut was free to bend in a fore and aft direction (using a flexure plate at its lower end) to allow for longitudinal thermal expansion. (Shorter struts were used during much of the assembly phase.)

Load cells on loan from NASA, Ames, were mounted between the model and the top end of the support struts. They measured normal and axial forces only. The left wing load cell was fixed, laterally, on its spindle (with spacers) and the other two load cells were allowed to 'float' laterally to allow for thermal expansion or other dimensional changes. The 'floating' capability of the free load cells was not particularly good, despite adequate lubrication, and some zero shift could be attributed to this cause but fortunately the magnitude was not great.

5.2 Test Operations

A test trailer was located about 100 feet from the model on its test rig and provided accommodation for an engine operator, and control console instrumentation personnel, recording equipment, etc. Electrical services and fuel supplies were available near by.

Weather conditions were generally cold and windy. Wind caused very noticeable changes in axial force measurements, due to momentum drag of the engine and augmentor inlet flows but no discernible effects in normal forces.

Screech from the circular trimming orifice nozzle, especially with the wing augmentor off when a larger diameter nozzle was required, was definitely noticeable at pressure ratios above about 2.0. (Maximum pressure ratio reached during the tests was 3.0.) Some attempts to alleviate it with reflection shields and small irregularities in the nozzle were partially successful.

5.3 Instrumentation

5.3.1 Engine Operator's Panel

The instrumentation complement was:

Exhaust gas temperature	(EGT °C)
Engine rpm gauge	(rpm %)
Oil pressure gauge	(psig)
Oil temperature gauge	(°C)
Fuel pressure gauge	(psig)
Vibration monitor	
Exhaust gas pressure gauge (PF1)	("Hg abs) (See below)

The usual engine controls were on the panel also.

5.3.2 Pressure Measurements

Static pressures were measured at the following locations (see Figure 8).

1) Fuselage duct inlet -

Static tap PF1 was read on a pressure gauge at the engine operators panel.

Static tap PF2, located close to PF1, was read on a pressure gauge and was also tee'd into the back face of a 50 psid transducer in a 48 port scanivalve.

2) Fuselage duct at the wing off-take location (P_W).

3) Fuselage duct near the rear trimming nozzle (P_N).

4) Wing duct statics (3), one in each bay of the left wing duct (PW1, PW2, PW3).

5) Fuselage augmentor throat; four locations near the throat on each wall of the left hand augmentor. A 'tape' of four stainless steel tubes perforated at the appropriate locations was attached to each wall of the augmentor, in between nozzles, near mid-length.

Total pressures were measured at

1) Fuselage augmentor nozzle exits, nozzle numbers 1, 2, 6, 12, 19 and 27 of the right hand augmentor, counting from the front. The pitot location was at about mid nozzle span.

2) Wing duct extremities, left and right sides.

Except for PF1 and PF2 all other pressures were measured with the scanivalve, differentially with respect to PF2. The S/V was manually stepped and output was displayed on a DVM.

5.3.3 Load Cells

Axial and normal force components read-out was on a manually operated digital strain recorder (Budd). Signal damping is under continuous manual control but S/N ratio was very good. Some zero shift appeared to be thermally generated, some was due to side loads imposed due to "stiction" on the load cell spindles.

6. RESULTS

6.1 J97 Running Line

Running limits for the J97 engine used in the VTOL model have been set at 705°C EGT (continuous operation) and 100% rpm. Ideally an effective nozzle area is chosen which allows both limits to be reached simultaneously at a given ambient temperature. This will produce the maximum exhaust pressure ratio. During the cold weather tests at DHC several nozzle sizes were used and EGT was the limiting boundary in most cases.

It is not possible to determine the absolute value of the effective nozzle area since the geometric areas of the fuselage and wing augmentors are not known accurately, (neither are the expansion effects due to pressure) and the discharge coefficient of the wing augmentor is not known. However, the approximate effective area is about 110 sq. ins., and the effect of a known, small, change in effective area was established. A set of running lines, expressed in the form EGP and ETR vs $N/\sqrt{\theta}$ was constructed (see Figure 9) and the temperature and rpm limits determined at various ambient temperature conditions. (The 40 x 80 foot wind tunnel at Ames has an operating temperature range from about 60°F to as high as 120°F typically). Figure 10 shows how variations in effective nozzle area affect the performance at various ambient temperatures. Figure 11 shows the optimum nozzle area for maximum exhaust gas pressure ratio as a function of ambient temperature.

6.2 Fuselage Augmentor Performance

The gross thrust augmentation ratio of the fuselage augmentor was determined from vertical force measurements with fuselage doors on and off. With doors 'on' the augmentor was complete; with doors 'off' a configuration was obtained which was basically 'nozzles plus inlet fairings plus fuselage side wall'. It had been determined from full-scale, cold flow tests on the DHC laboratory outdoor test rig, that this configuration gave a thrust force approximately 10% greater than the nozzles alone (see Figure 12). Assuming that this rather small effect of inlet fairings would be the same with the hot exhaust gas of the J97-powered model, then the hot nozzle thrust can be determined from the 'doors off' test.

Two small effects preclude simply taking the ratio of 'doors on' force to nozzle thrust as gross thrust augmentation ratio. The first is the increase of mass flow through the nozzles when the fuselage doors are on - this is due to the lowered static pressure, in the region of the nozzle exit, increasing the actual nozzle NPR. Laboratory tests showed a small increase in nozzle flow rate even above choking pressure ratio, due to a small effect of NPR on discharge coefficient. The second effect is due to the presence of a fuselage base pressure causing a base pressure thrust. A small negative pressure was measured at a single location on the base, showing that the model was essentially out of ground effect.

Both effects have been taken into account in the data presented in Figure 13. The derived gross thrust augmentation ratio is given in Figure 14 compared with the large scale, cold flow laboratory tests. At the higher pressure ratios, where the high level of measured forces allows greater accuracy, the agreement is very good and indicates only a small deleterious effect presumably due to a high gas temperature.

The measured augmentor throat wall static pressures indicated a local Mach number of 0.56 at NPR = 3.0. This is somewhat less than anticipated and suggests that some improvement in augmentation ratio is still possible by increase in exit area.

6.3 Wing Augmentor Performance

Only augmented thrust of the wing nozzles was measured during the present tests. It is hoped that 'shrouds off' tests will be possible some time during the wind tunnel tests and, if not, certainly during the static test program at Ames following the tunnel tests.

The increment in vertical thrust due to rotating the wing augmentors from $\delta_W = 0^o$ to $\delta_W = 90^o$ is shown in Figure 15 and compared with the estimated wing nozzle thrust. Due to inadequate knowledge of nozzle area and discharge coefficient the nozzle thrust is not predictable accurately but test results imply that the nozzle thrust is greater than expected. The anticipated gross thrust augmentation ratio, based on laboratory tests, was 1.60 at NPR = 3.0. (The test results show ϕ_G about 10% greater than this at maximum NPR.)

6.4 Duct and Nozzle Pressure Losses

Static pressure taps were used at a number of locations in the ducting system, as shown in Figure 7, and total pressure taps were fitted at the exits of six of the fuselage augmentor nozzles (Figure 5). Typical values for these pressures in terms of the reference pressure PTN are shown in Figure 16.

The highest pressure was measured at the rear fuselage duct location when the orifice (trim) nozzle area was small. Then, static pressure in the duct (PN) was equal to total pressure (PTN) since duct Mach number at that location was negligible. Compared with the derived total pressure at the duct inlet (PTF), derived from an approximate knowledge of the J97 mass flow and the measured static pressure, PF1 or PF2, it would appear that PF is unexpectedly low. Possible explanations include high initial swirl in the J97 exhaust and/or a very non-uniform total pressure distribution at the duct inlet - the latter is most likely.

If PTN is taken as the average duct inlet total pressure then the loss at the fuselage augmentor nozzle exit plane is about 5 1/2% for the first nozzle and about 4% for the rest of the nozzles.

The corresponding pressure drop from PTN to the tip of the wing ducts was about 2%. No measurements were made at the exit plane of the wing augmentor nozzles.

6.5 Overall System Performance

The estimated maximum thrust of the J97 used in the VTOL model was 4900 lb. This assumes that the ideal nozzle area is chosen which causes both temperature and rpm limits (705°C and 100% respectively) to be reached simultaneously at standard day conditions. (The thrust data came from a simple test rig at Ames Research Center prior to tests at DHC.)

The normalized total thrust of the VTOL model was obtained from Run 9, where the wing augmentor was deflected to 90°. The small trimming nozzle thrust was added to the vertical thrust to give total thrust. The data included small corrections for fuselage base thrust and load cell interaction effects.

Despite the VTOL model nozzle area being slightly too small for standard day conditions (see Figure 11) an overall ratio of model thrust to bare engine thrust of 1.52 was achieved (Figure 17). The model thrust at NPR = 3.0 was apportioned as follows:

Fuselage augmented thrust	73.6%
Wing augmented thrust	23.5%
Rear trimming nozzle	2.9%
Total	100.0%

The base thrust amounted to about 0.4% of the total thrust. This is somewhat less than expected from previous test data.

The ratio of augmented wing thrust to augmented fuselage thrust is 0.32. The original target figure was 0.25 but the optimum division of thrust is not yet known.

Using the above division of thrusts and the overall thrust ratio of 1.52 together with the measured thrust augmentation ratios and duct pressure losses, it appears that there must have been about 4% pressure loss between the engine proper and the duct pressure PTN. Most of this would likely occur in the convergent/divergent connecting duct (see Figure 8).

7. CONCLUSIONS

(a) No structural failures occurred after 10 starts and about 4 hours of running.

(b) Engine bay temperatures were less than 150°F when the ambient temperature was about 35°F.

(c) The fuselage augmentor produced a gross thrust augmentation ratio of 1.60 at NPR = 3.0. This compares with 1.66 for the cold flow tests of an identical configuration - the difference is believed to be due to the respective primary flow stagnation temperatures.

(d) The wing augmentor thrust augmentation ratio was not determinable from the tests performed but appeared to be at least as high as expected, i.e., about 1.60.

(e) Total pressure loss in the duct system, from the maximum reading in the fuselage duct to the fuselage augmentor nozzle exit plane, was about 4% of the absolute total pressure.

(f) Further static tests are required to define the effects of diffuser area ratio and height above ground.

8. REFERENCES

1. Whittley, D.C. "Some Experimental Research on a New Aircraft Configuration Incorporating Ejector-Type Thrust Augmentation for VTOL"

   ICAS Paper No. 70-56, Rome, September 1970.

2. Garland, D.B. "Description and Test Specification for the J97 Powered External Augmentor VSTOL Wind Tunnel Model"

   DHC-DND 77-3. December 1977.

TABLE 1 GEOMETRY OF J97 POWERED, EXTERNAL AUGMENTOR V/STOL MODEL

Wing	
Area, gross	141 ft^2
Area, net	97 ft^2
Span	15.25 ft.
Aspect ratio	1.65
t/c	6%
m.a.c.	12.68 ft.
Chord on fuselage ℄	16.92 ft.
Fuselage	
Overall length	approx. 28 ft.
Fin	
Area	22.4 ft^2
Span (above fuselage top)	4.33 ft.
Aspect ratio	0.84
Tailplane	
Area	20.4 ft^2
Span	7.67 ft.
Aspect ratio	2.88

Moment reference centre (wing leading edge joint, on wing chord datum)
Distance ahead of rear strut location $\bar{x}$ = 44.0"
(also equal to 47.2% of m.a.c.)

TABLE 2 GEOMETRY OF FUSELAGE AUGMENTOR

Augmentor	
Chordwise length	= 98 in.
Throat width (L_T)	= 10.5 in.
Exit width (L_E)	= 16.8, 10.5 in.
Diffuser area ratio (L_E/L_T)	= 1.60, 1.00
Length (min) (L)	= 34 in.
Mean nozzle width ($\bar{t}$)	= 0.457 in
Augmentor length ratio ($L/\bar{t}$)	= 74
Nozzles	
Total geometric exit area (per side)	≈ 45.7 in^2
Number of nozzles (per side)	= 27
Area (per nozzle)	= 1.693 in^2
Aspect ratio (AR)	= 60
Span (b_N)	= 10.12 in.
Thickness at exit (t_N)	= 0.167 in.
Pitch (p)	= 3.68 in.
Pitch ratio ($p/\bar{t}$)	= 8.0

Note: Clearance between end nozzles and augmentor end-walls is 1/4p when hot.

TABLE 3 GEOMETRY OF WING AUGMENTOR

Span (per wing)			= 69.5 in.
Total nozzle area (per wing)			= 11.5 in^2
Bay spans	24.25	22.75	22.5 in.
Nozzle area/bay	4.88	3.73	2.88 in^2
$\bar{t}$	0.201	0.164	0.128 in.
Number of nozzles (N)	15	17	22
Area per nozzle (A_N)	0.325	0.219	0.131 $in.^2$
Pitch (p)	1.60	1.32	1.01 in.
Nozzle span (b)	3.61	2.96	2.29 in.
Nozzle thickness (t)	.090	.074	.057
Nozzle aspect ratio (AR)	40	40	40
Throat (mid span) (L_T)	4.17	3.40	2.65
Exit (mid span) (L_E)	6.67	5.44	4.24
Diffuser area ratio L_E/L_T	1.60	1.60	1.60
Nozzle inlet area/exit area	5.0	5.0	5.0
Augmentor length (mid span) (L)	17.3	14.7	12.1
$L/\bar{t}$	86	90	95

TABLE 4

RUN HISTORY OF STATIC TESTS AT DHC

Run No.	Rear Orifice Nozzle Diameter	Remarks
001	8.75"	Wing augmentor off. Cowlings off. Augmentor doors on.
002	"	"
003		Aborted due to throttle malfunction.
004	6.21"	Reduced distance between nozzles and augmentor end walls (to 1/4 pitch).
005	"	Anti-screech shield added to rear nozzle. Augmentor throat surface roughness removed.
006	"	. "
007	"	Augmentor doors removed. End walls retained. Anti-screech shield replaced with 0.75 in^2 'mouse' in orifice nozzle.
008	2.80"	Wing augmentors added. $\delta_W = 0^\circ$. Fuselage augmentor doors on. No fairings between wing and wing augmentor. Load cell lateral clearances increased.
009	"	δ_W - 90°. Bay cowling vent covers on.

DHC EXTERNAL AUGMENTOR V/STOL CONCEPT

G.A. OF J-97 POWERED MODEL

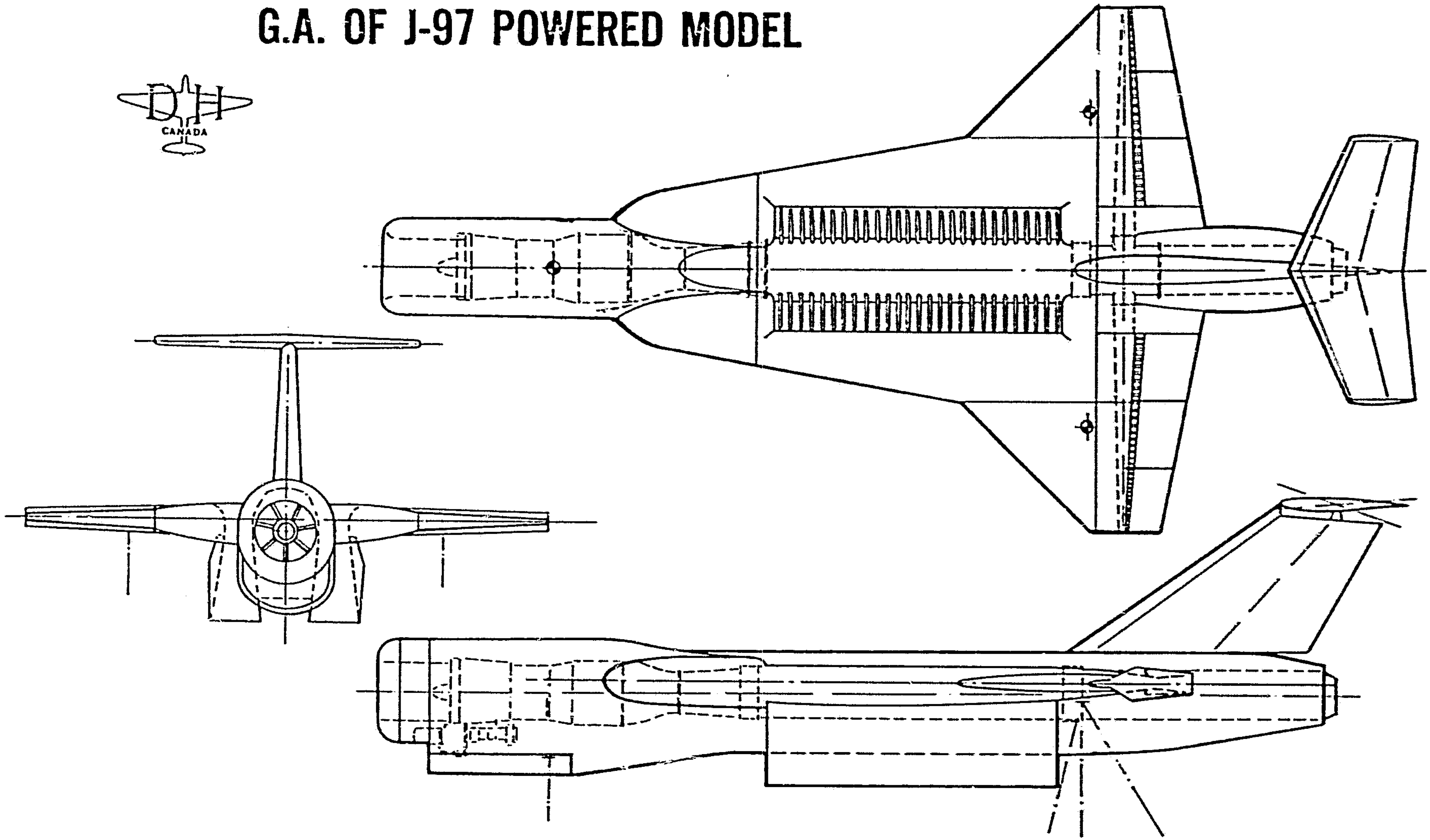

Fig. 1

D H CANADA

Fig. 2

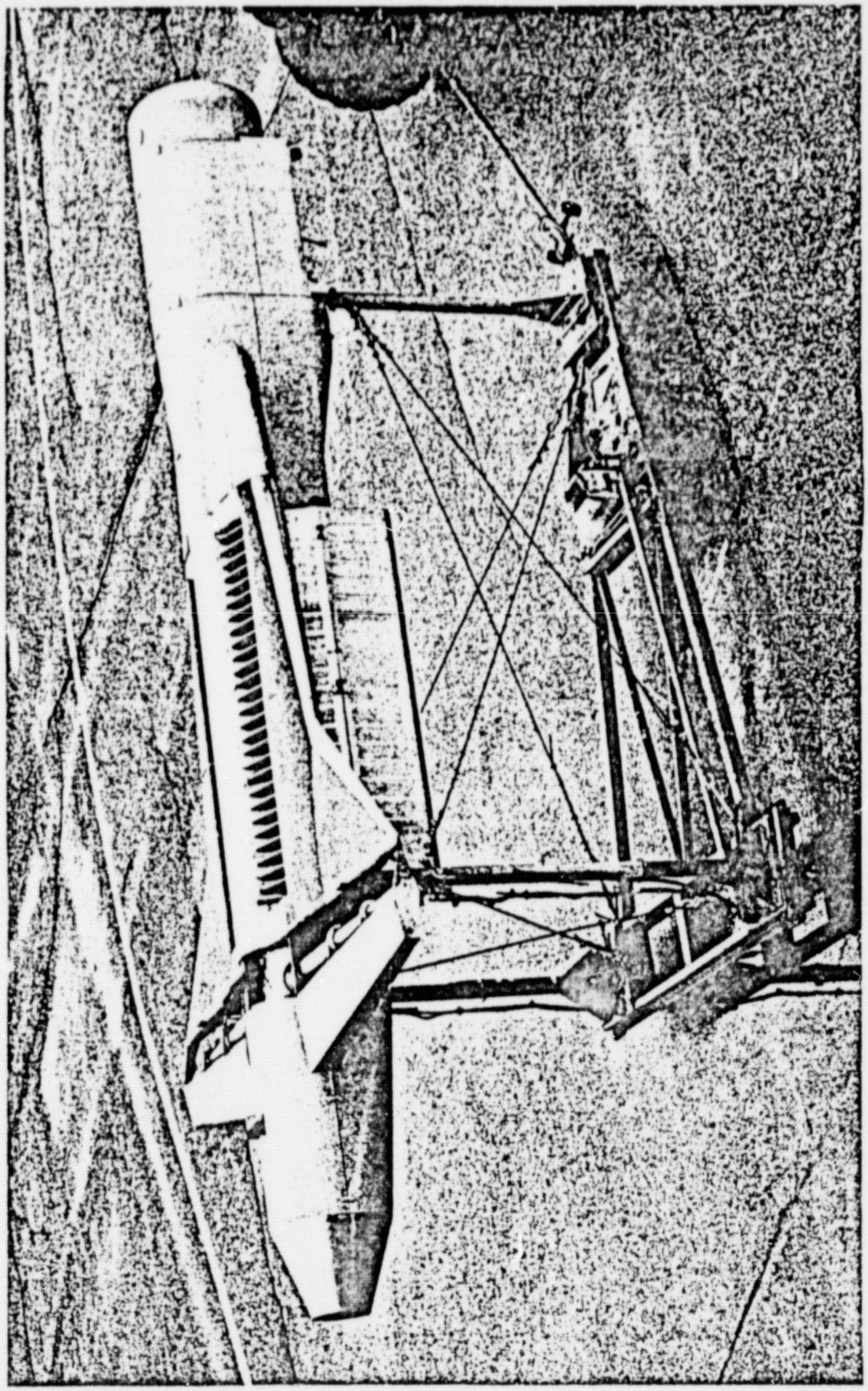

J97 POWERED VSTOL MODEL ON STATIC TEST RIG

Fig. 3

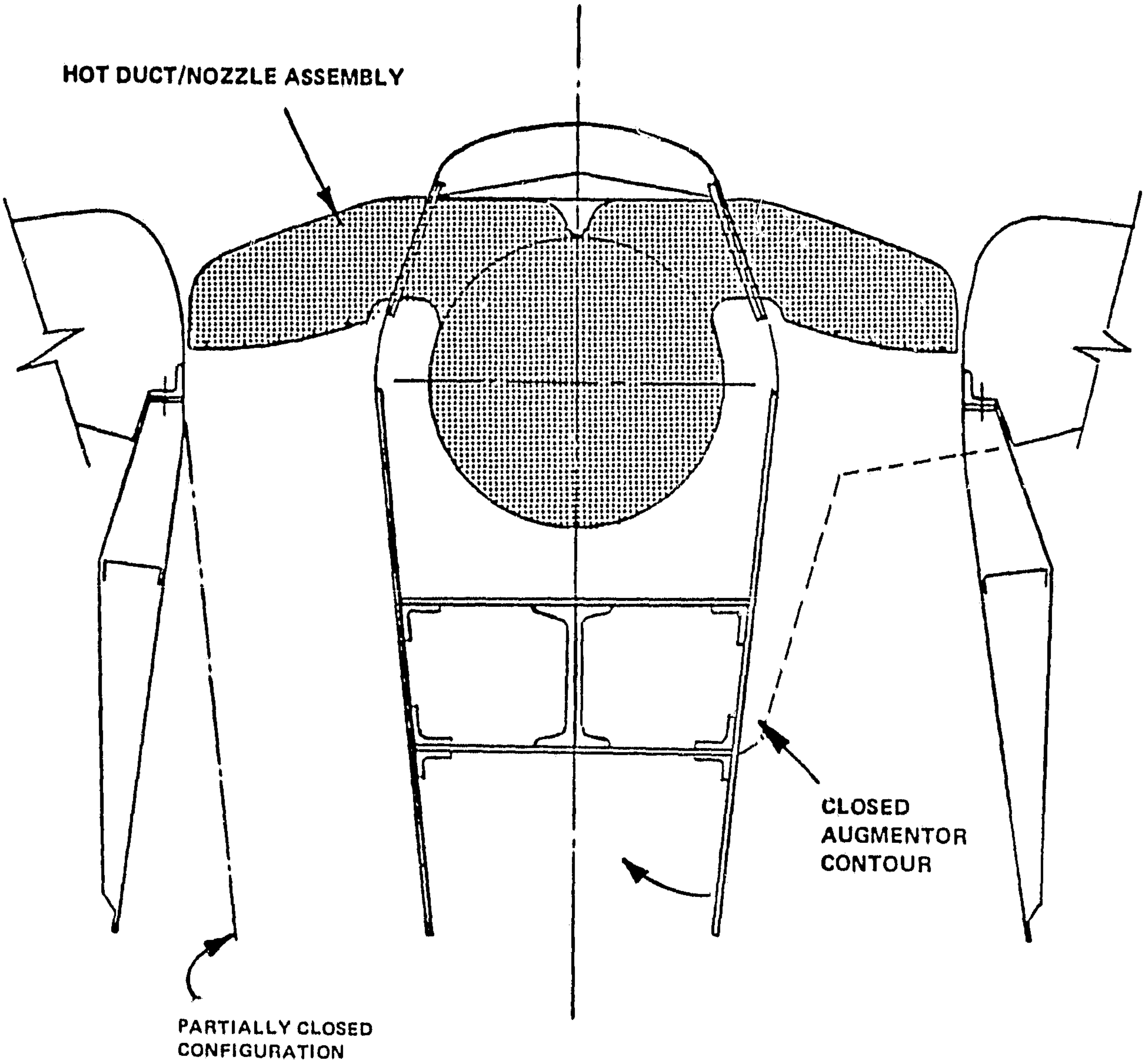

SECTION THROUGH FUSELAGE AUGMENTOR

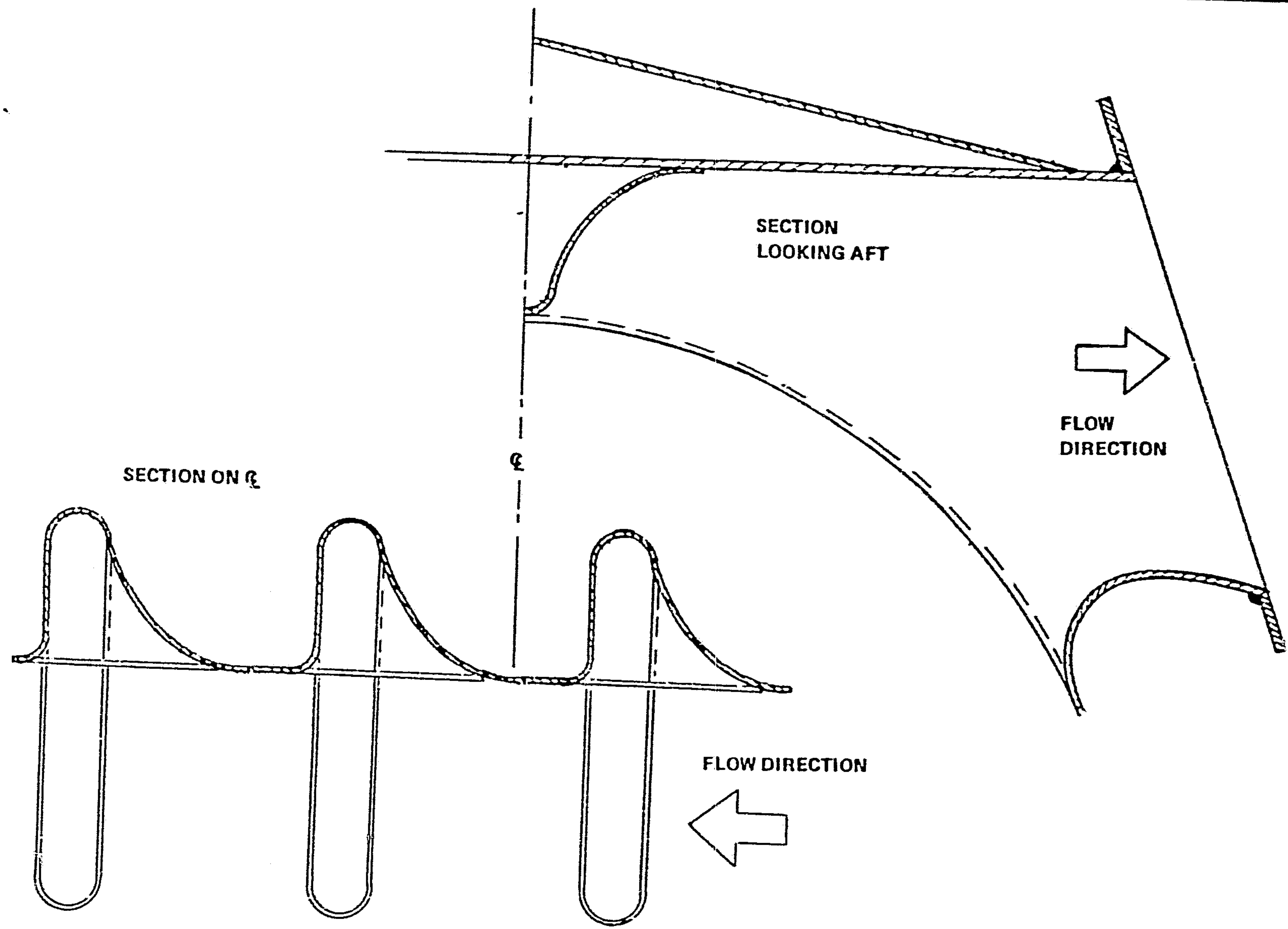

FUSELAGE AUGMENTOR NOZZLE OFFTAKES

Fig. 5

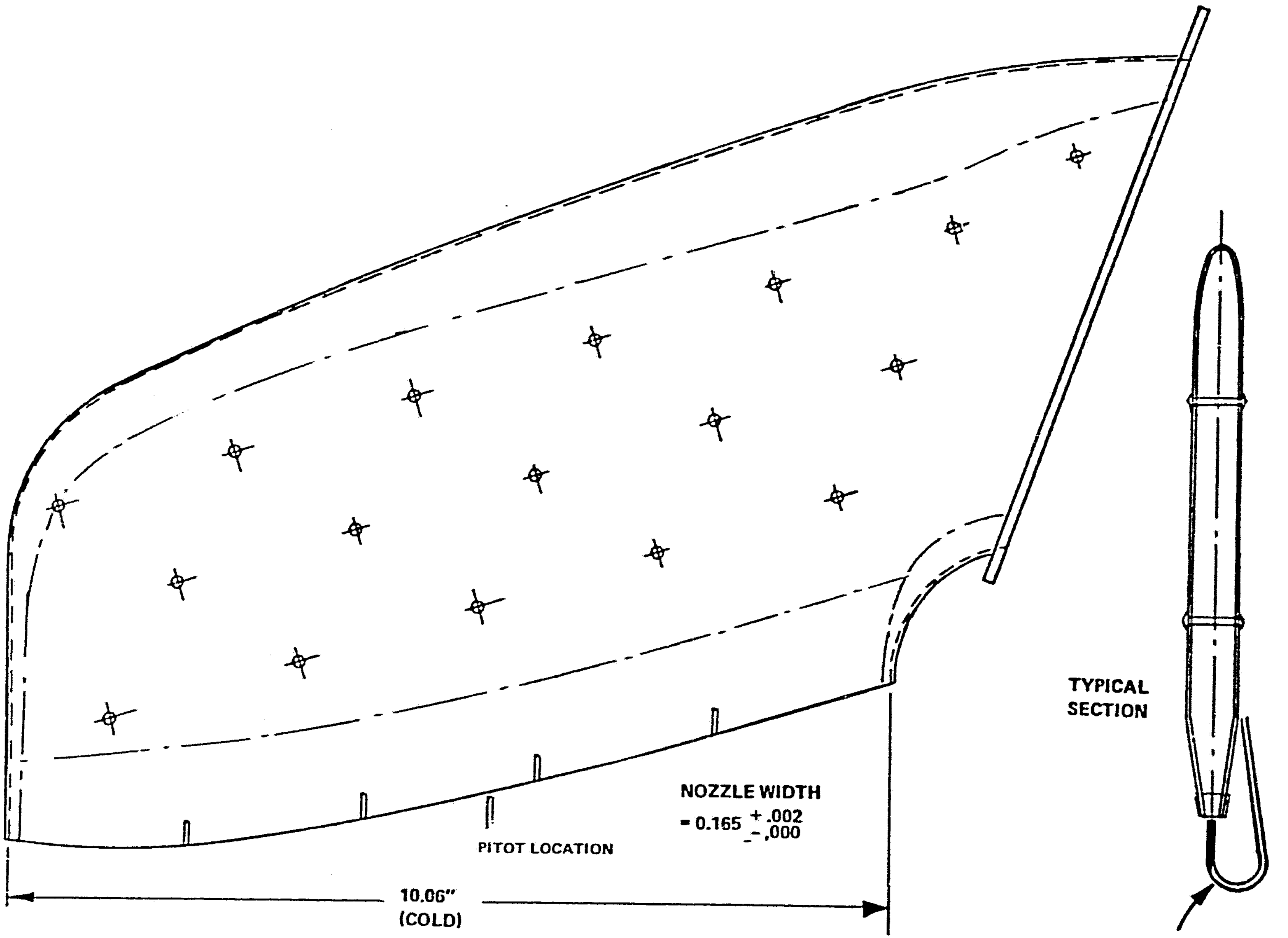

FUSELAGE AUGMENTOR NOZZLE

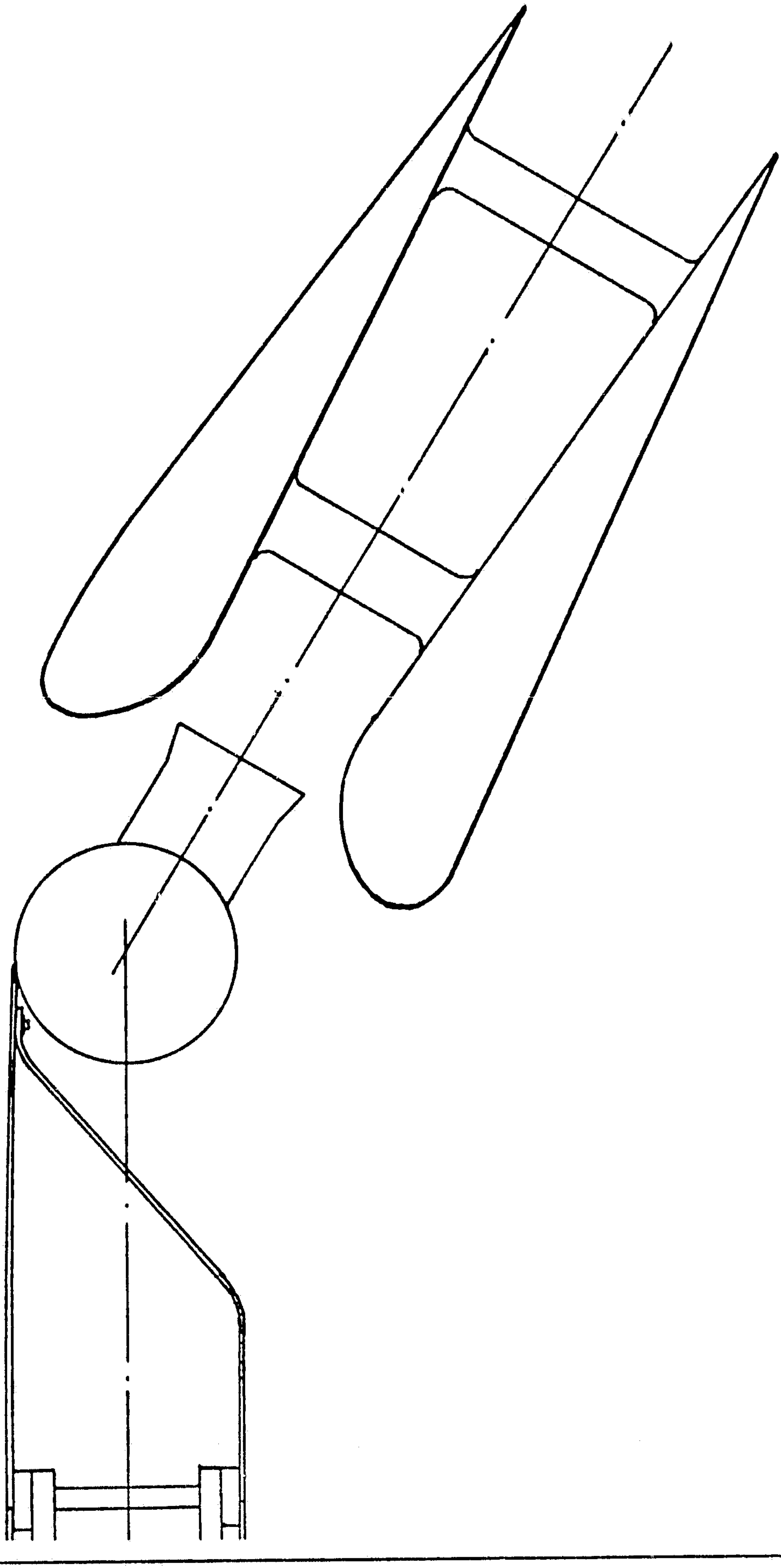

SECTION THROUGH WING AUGMENTOR FLAP

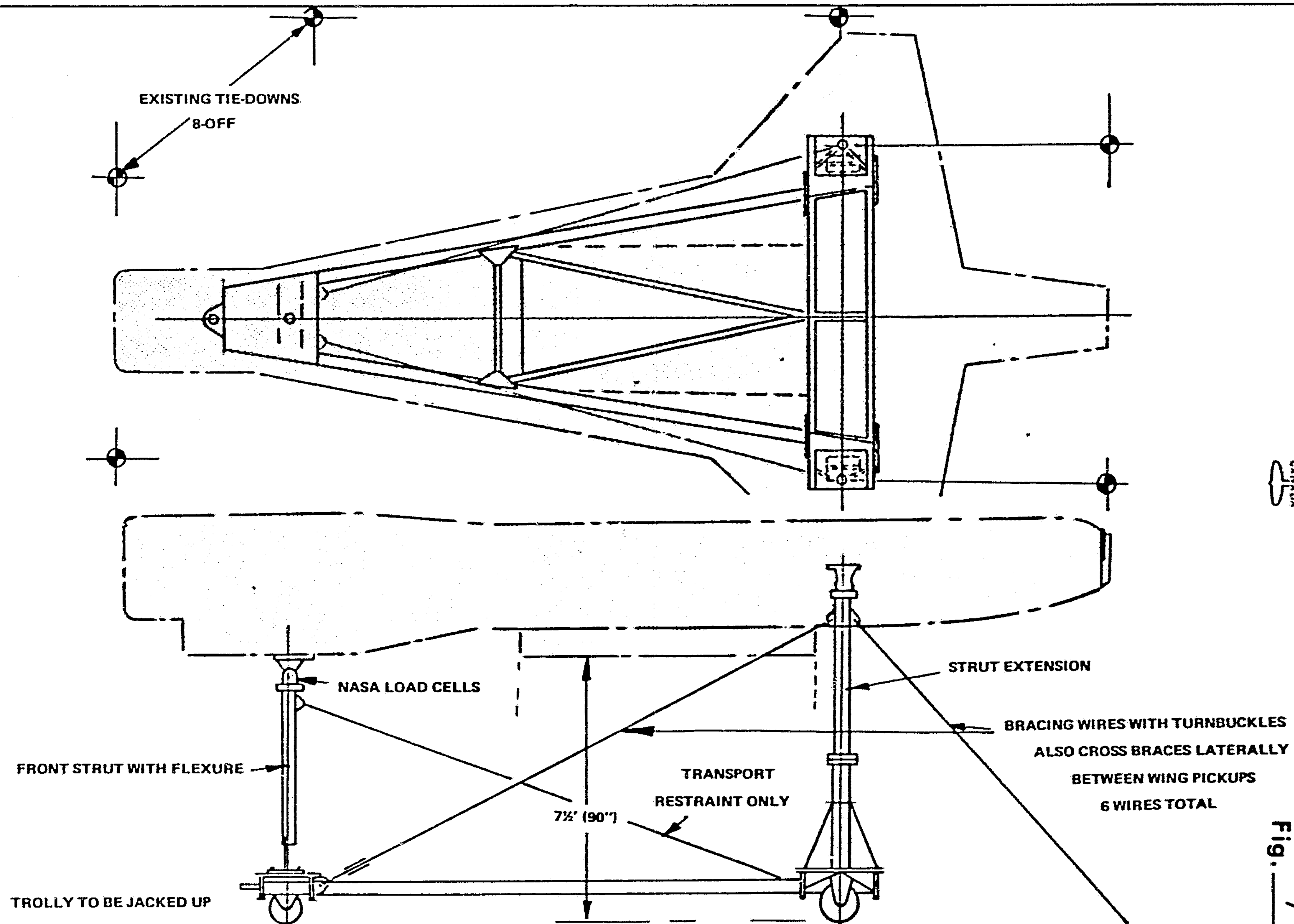

TEST CONFIGURATION

Fig. 7

Fig. 8

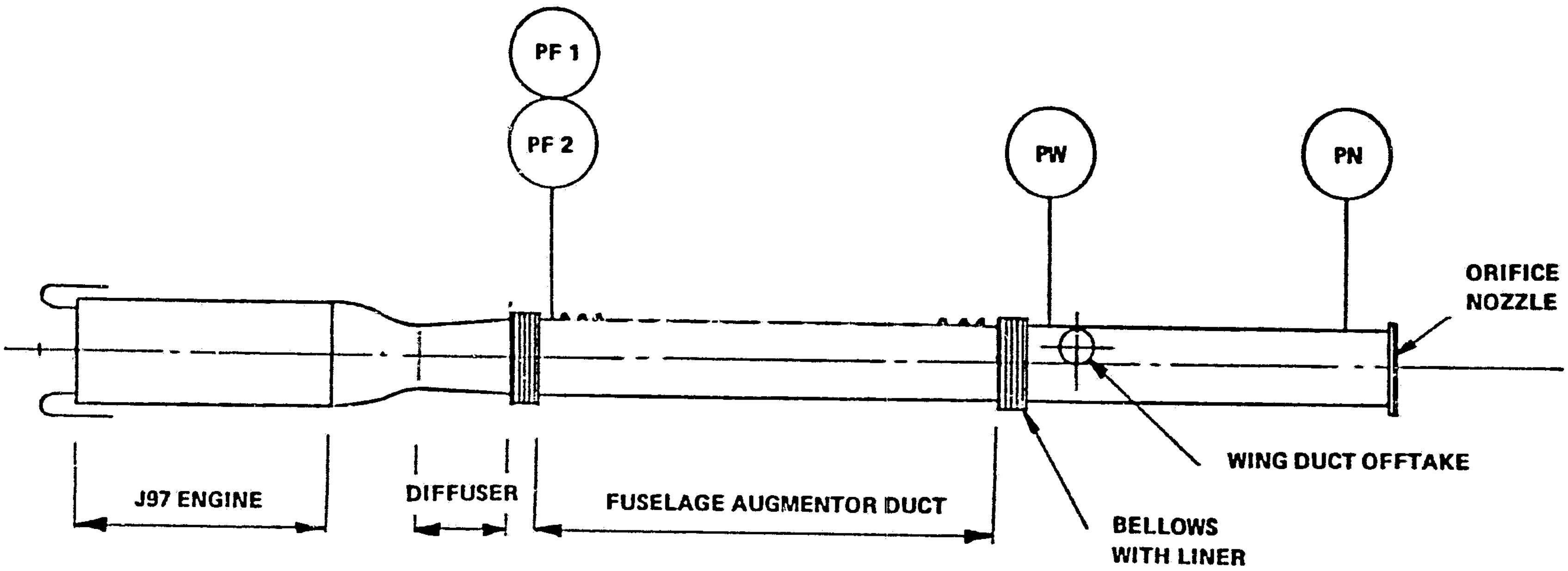

LOCATION OF DUCT STATIC PRESSURE TAPS

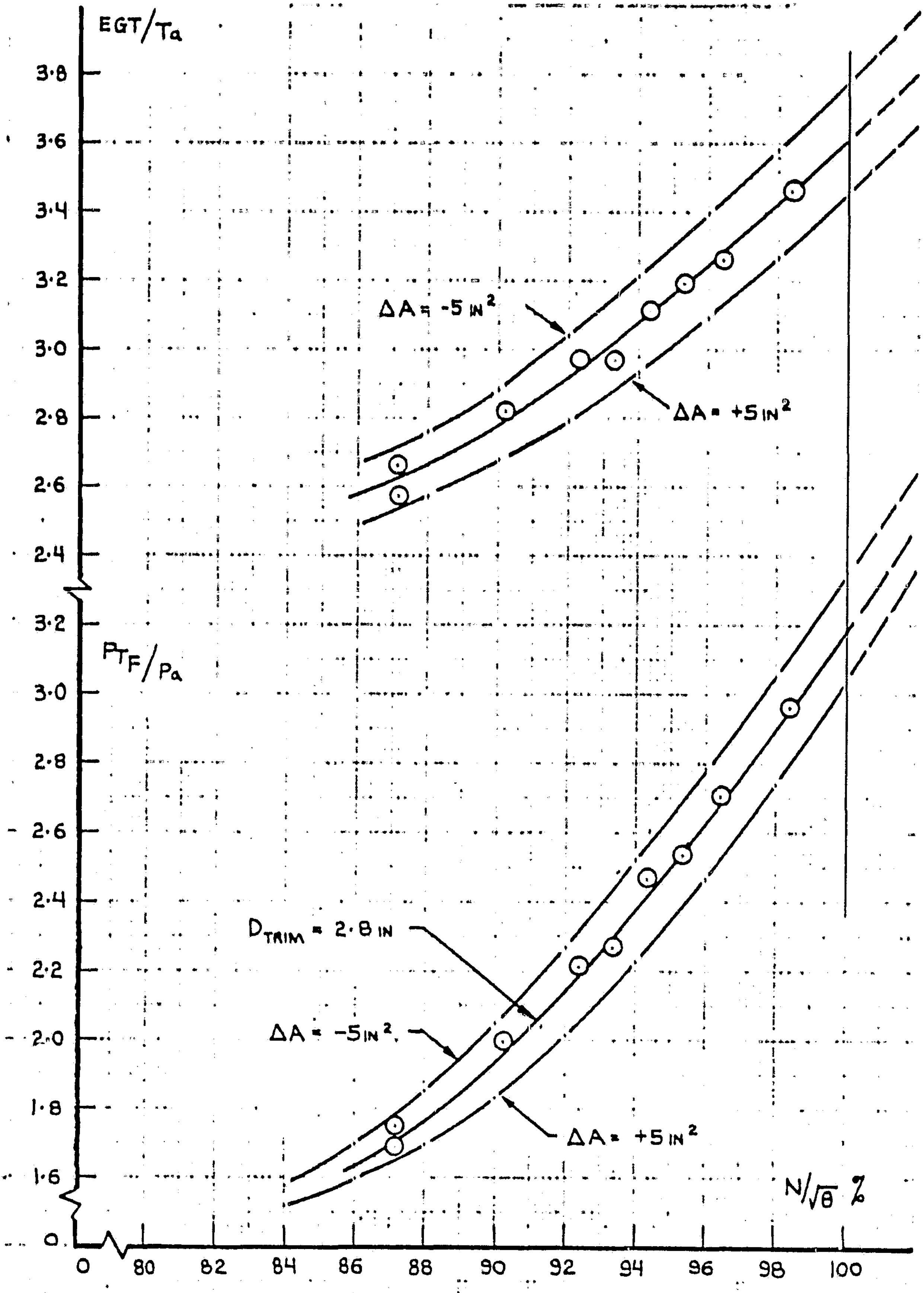

EFFECTS OF NOZZLE AREA ON J97 PERFORMANCE

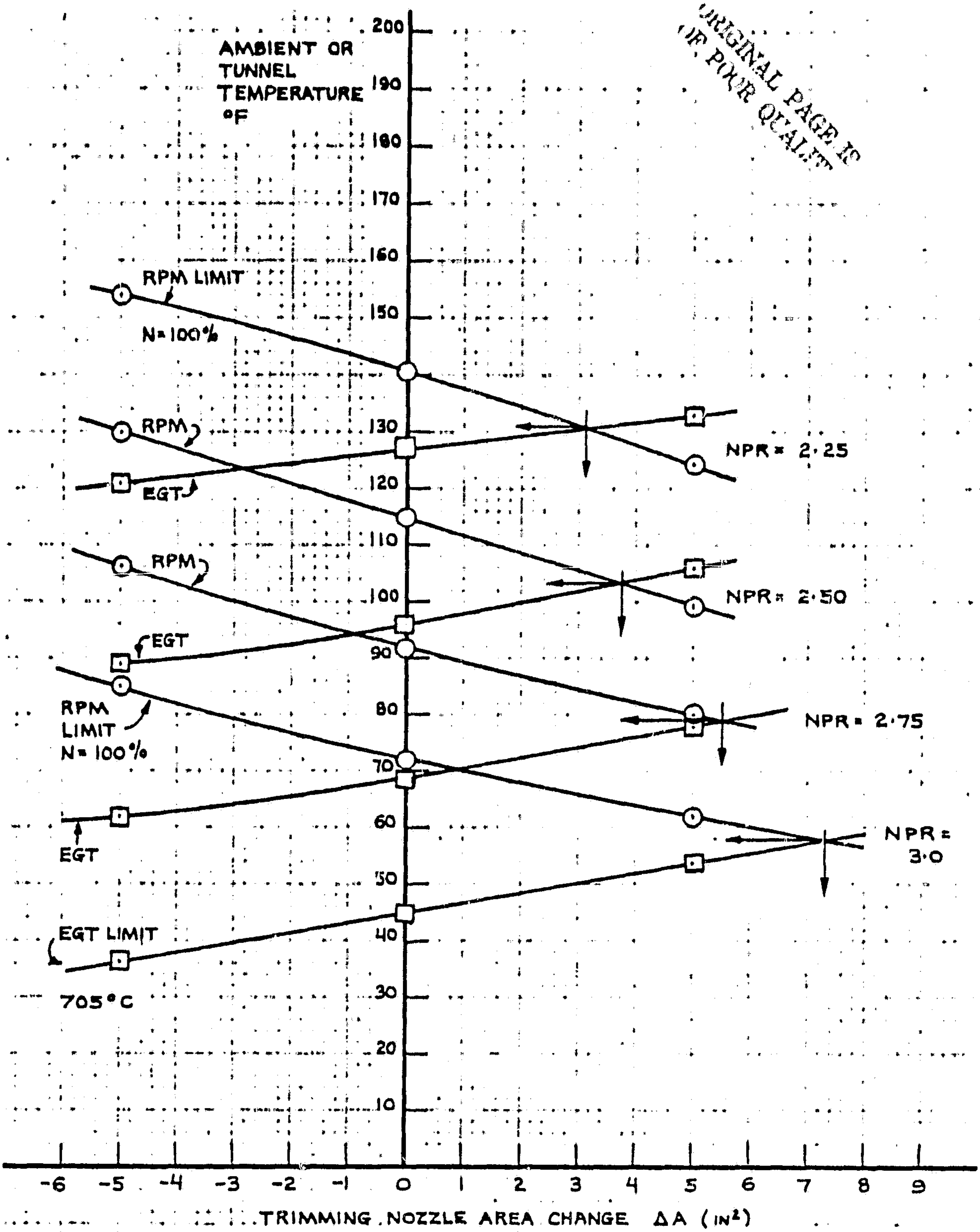

RPM — EGT LIMITS ON J97 PERFORMANCE VS TRIMMING NOZZLE AREA CHANGE RELATIVE TO EXISTING 2.80" DIA TRIM NOZZLE

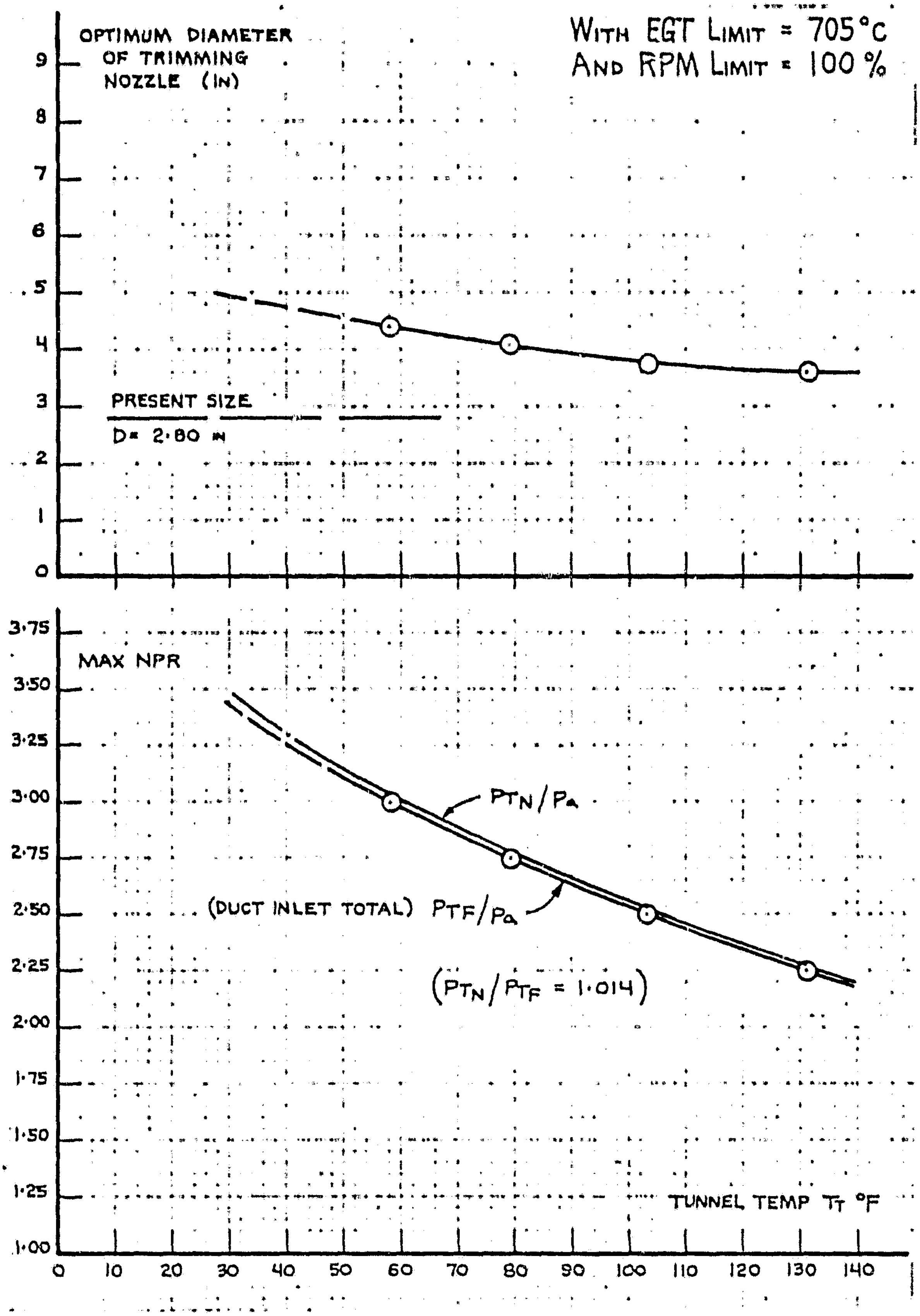

MAXIMUM AVAILABLE PERFORMANCE OF J97

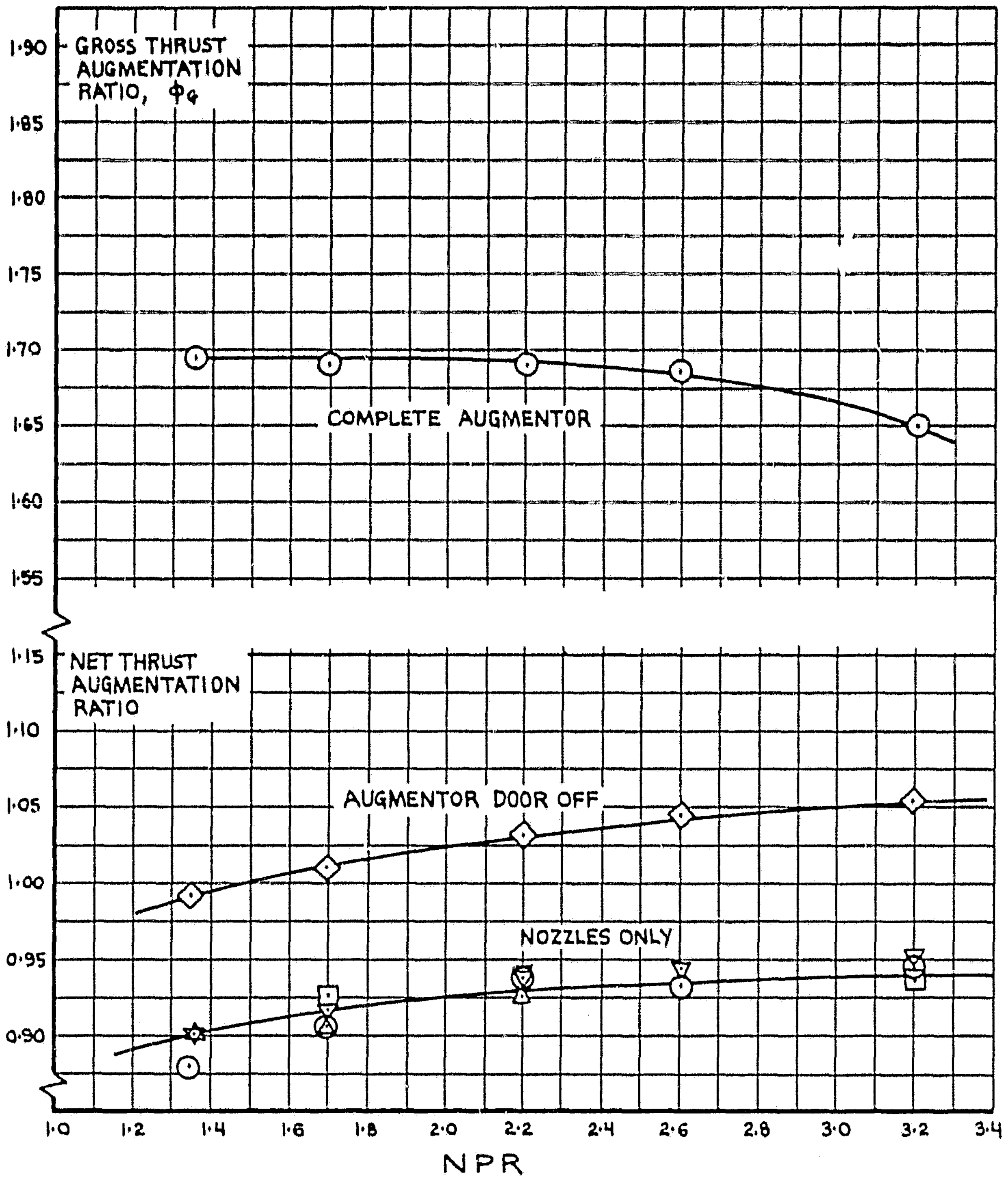

COLD FLOW VTOL MODEL TEST RESULTS

Fig. 13

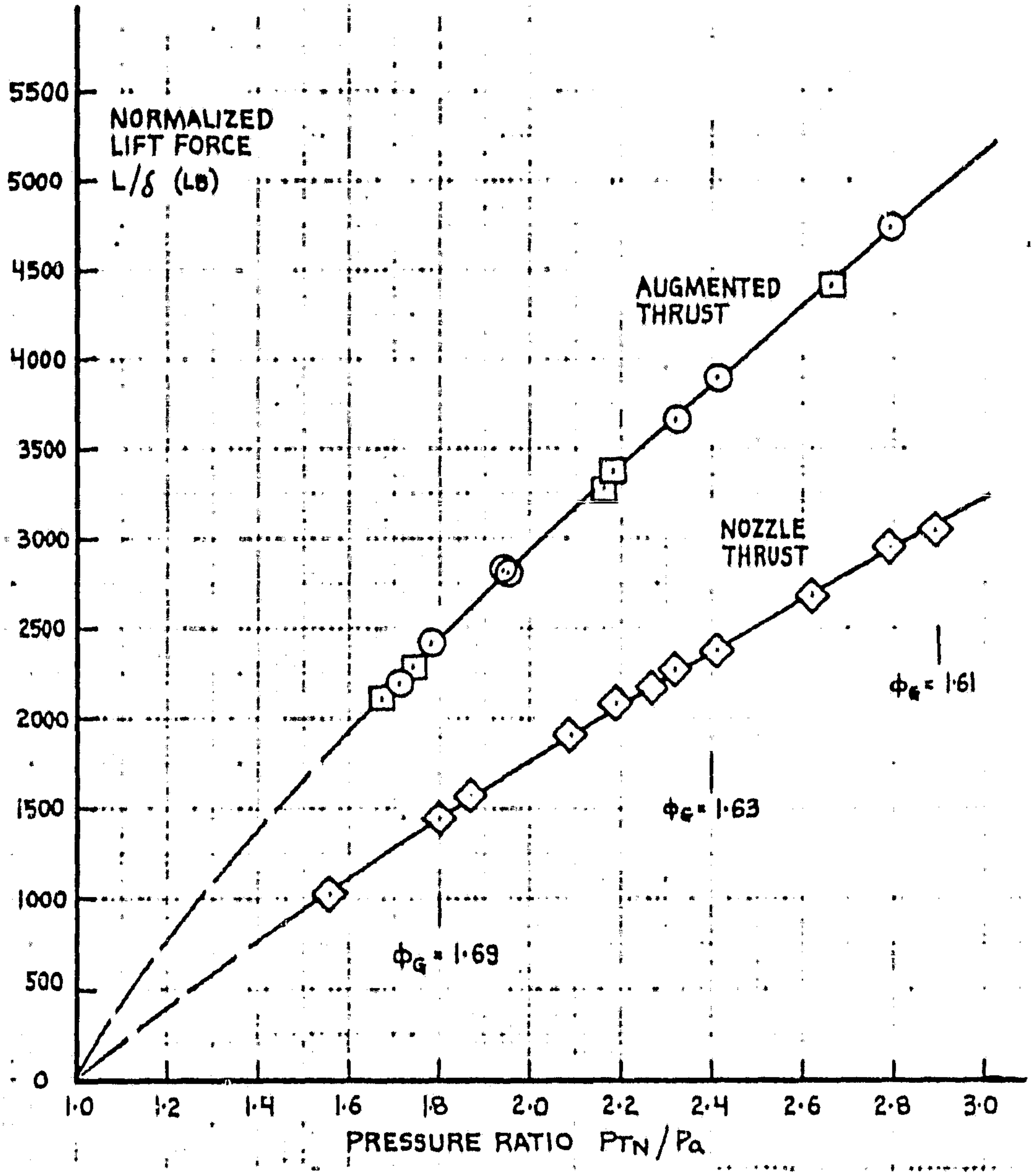

PERFORMANCE OF FUSELAGE AUGMENTOR

Fig. 14

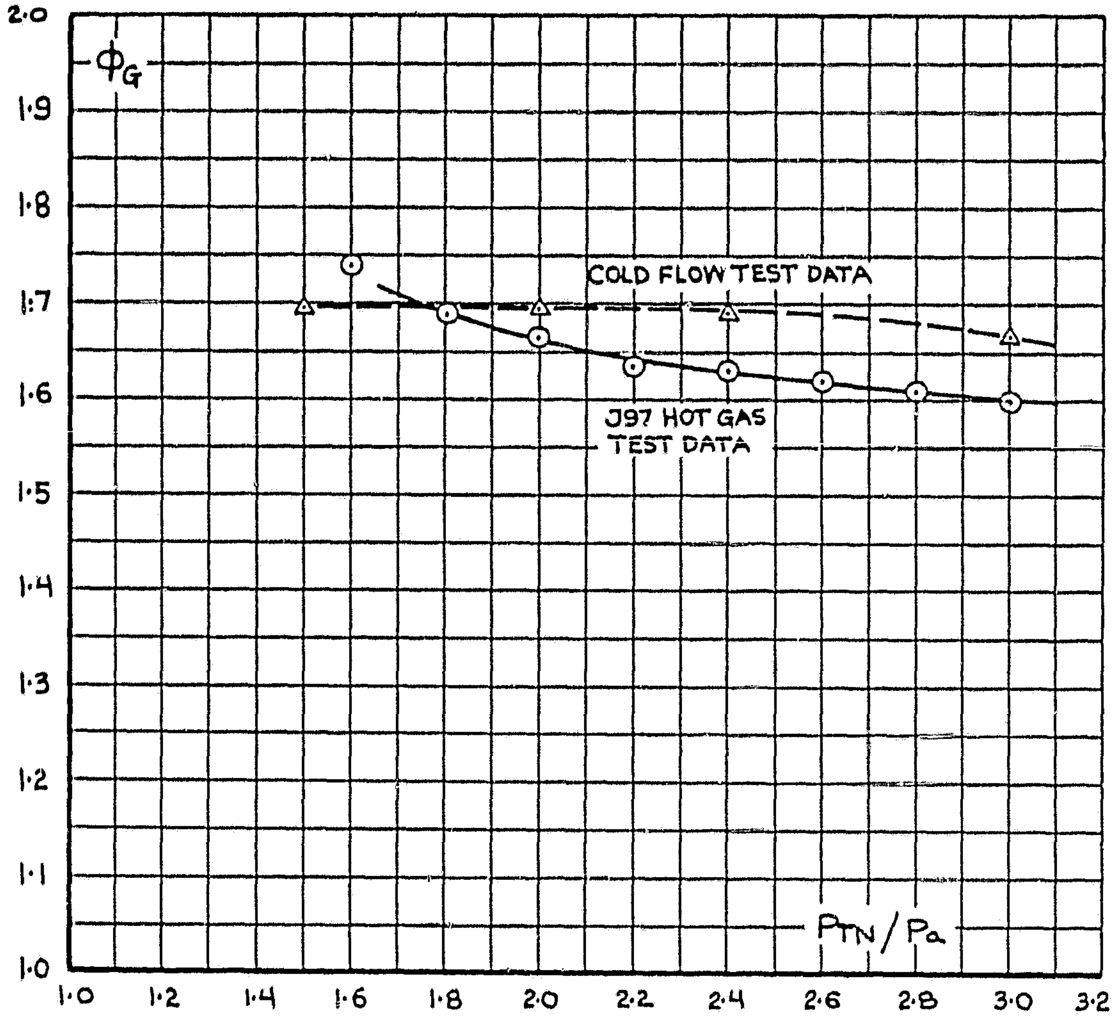

GROSS THRUST AUGMENTATION RATIO
OF FUSELAGE AUGMENTOR

Fig. 15

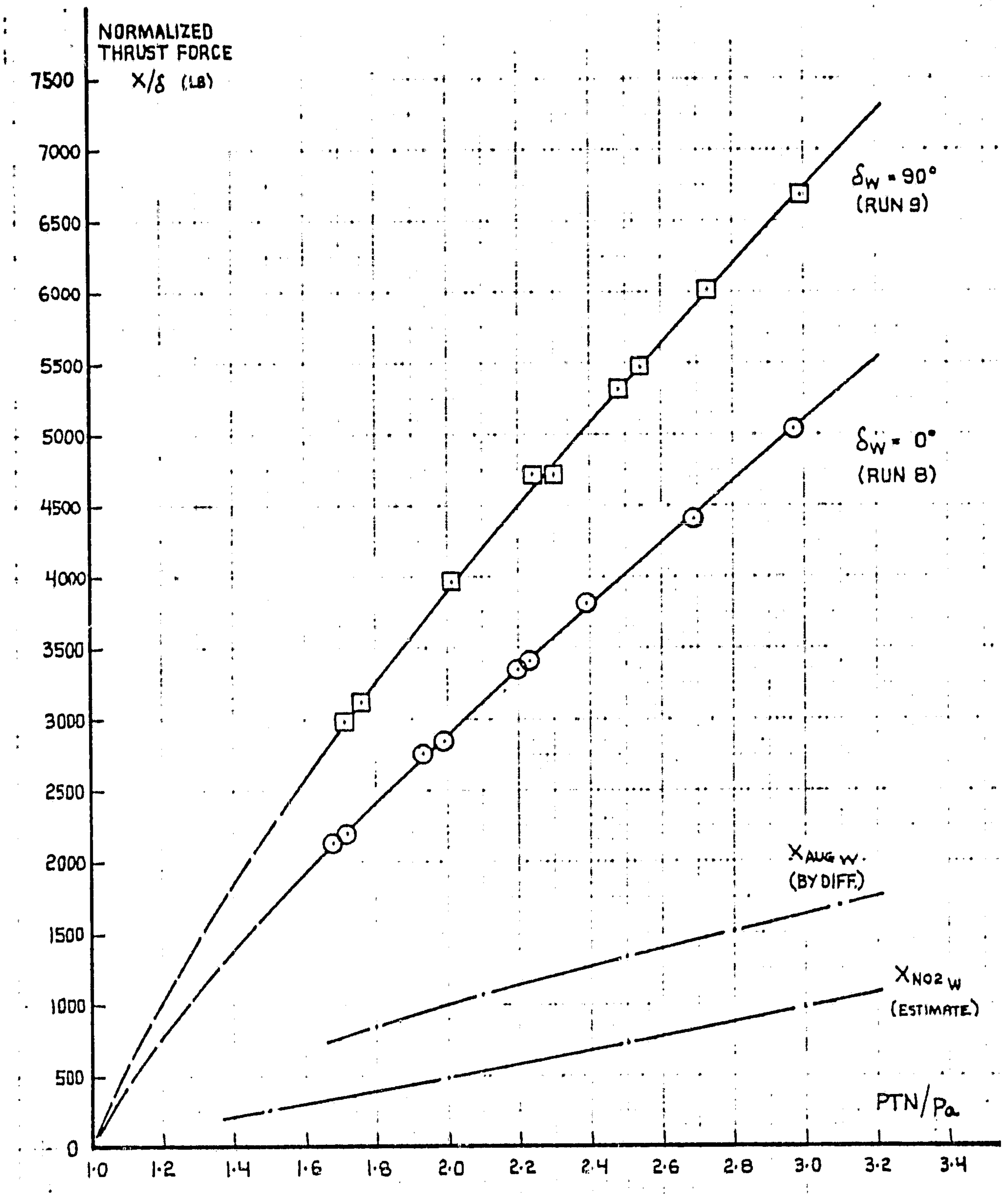

THRUST GENERATED BY WING AUGMENTOR

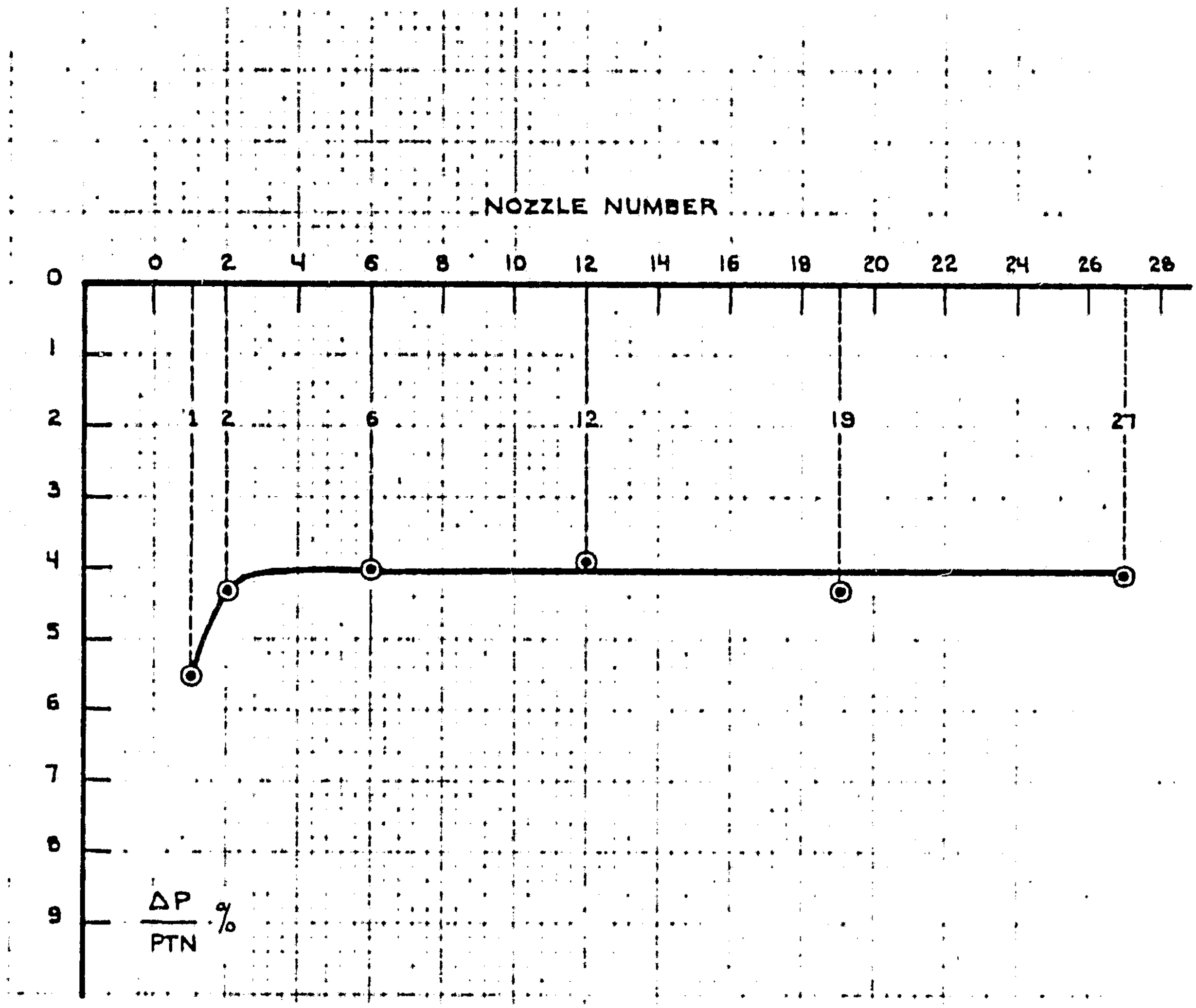

TOTAL PRESSURE LOSS BETWEEN FUSELAGE DUCT AND FUSELAGE AUGMENTOR NOZZLE EXIT PLANE

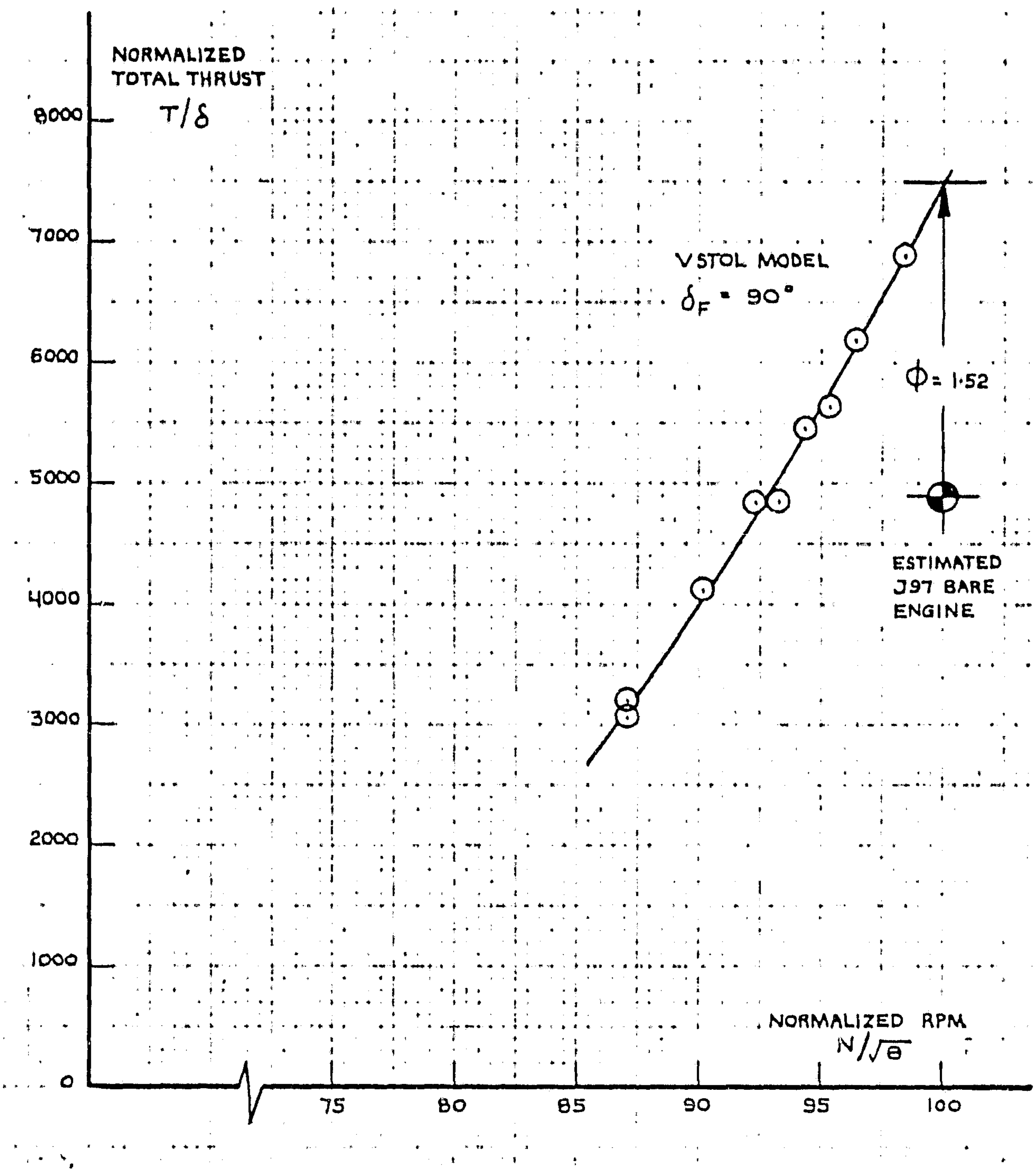

RATIO OF TOTAL THRUST TO INSTALLED THRUST.